20th Australasian Fluid Mechanics Conference
Perth, Australia
5-8 December 2016

Turbulent boundary layers developing over rough surfaces: from the laboratory to full-scale systems

N. Hutchins[1], J. P. Monty[1], B. Nugroho[1,2], B. Ganapathisubramani[2], I. K. A. P. Utama[3]

[1]Walter Bassett Aerodynamics Laboratory, Department of Mechanical Engineering
University of Melbourne, Victoria 3010, Australia

[2]Faculty of Engineering and the Environment
University of Southampton, Southampton, SO17 1BJ, UK

[3]Department of Naval Architecture and shipbuilding Engineering,
Institut Teknologi Sepuluh Nopember, Surabaya, 60111, Indonesia

Abstract

An overview of recent work on the problem of turbulent boundary layers developing over surface roughness will be given. This includes experimental laboratory studies, numerical simulations and recent attempts at full-scale in-situ measurements on the hull of an operating ship. The overarching aim here is to be able to make full-scale predictions of the penalty (economic / environmental / performance) resulting from surface roughness on the hulls of operating ships. This roughness could be due to the build-up of marine organisms on the hull of the ship or due to the surface finish attained during the hull coating process. For a given surface topography of interest, a key element to making these full-scale predictions is the ability to determine the equivalent roughness height (which is a measure of the degree to which the surface topography affects the flow). Several methods of estimating this roughness height will be discussed as well as a methodology for using this to obtain full scale predictions. Finally, a direct method will be presented for inferring the roughness penalty from an *in-situ* measurement of the boundary layer over the hull of an operating ship. .

Introduction

Many practical wall-bounded flows will occur at high Reynolds number. This is certainly true of aerospace and maritime applications, as well as meteorological and hydrological flows. High Reynolds numbers ensure that these boundary layers are predominantly turbulent and also raise questions about the dynamic smoothness of the solid boundaries. For any vehicle that moves through a fluid, or indeed any situation where flow moves over a solid boundary (i.e atmospheric boundary layers, or duct flows) the optimal surface condition in terms of minimising skin friction drag will almost always be a smooth finish. [1] The degree of smoothness required to meet this optimum condition is determined by the operating conditions (the flow speed and kinematic viscosity of the fluid), hence the commonly coined phrase aero- or hydro-dynamically smooth. As a result of high Reynolds numbers, the requirements for dynamic smoothness become, in most cases, unrealistically stringent. As an example, for a ship cruising at 15 knots (7.7 ms^{-1}), the maximum permissable equivalent sand grain roughness [20] for hydrodynamic smoothness is approximately 20 μm (less that the diameter of a human hair). Surface imperfections above this level will lead to a roughness modified turbulent boundary layer, with associated increases in wall drag and degradation in performance. Such surface finishes are not possible for most maritime applications (with the exception perhaps of racing yachts), and even the raw antifouling or foul-release coating on a new ship will often exceed this measure by a significant amount [25]. For the atmospheric surface layer the maximum permissable height is O(500 μm), which again is only very rarely achieved (perhaps over some salt playa deserts, or still water). Even for aircraft, where manufacturing tolerances are much tighter, the surface finish requirement for aerodynamic smoothness, which is O(20μm), is questionable. Though aircraft manufacturers will readily claim that this criteria is satisfied by the paint finish [12], the roughness of the fuselage and aircraft is not composed solely of painted smooth surfaces. Panel joints and rivet rows, though typically bundled together under the umbrella term 'excrescence drag' by the aerospace engineering community, represent roughness elements. In addtion, leading edges, and areas of the fuselage in proximity to the undercarriage will often become roughened by insect strikes and debris.

Hence, surface roughness is the norm in many practical wall-bounded flows, leading to substantial increases in drag and associated penalties (performance, energy expenditure, emissions and of course economic). Marine transport provides a sobering example of this penalty. The global shipping industry has a large environmental and economic footprint. There are estimated to be over 90,000 ships operating worldwide, together consuming approximately 5 - 7 million barrels of oil per day (up to 8% of the worlds production) [8]. The oil that these ships burn is mostly of a low grade (with a sulphur content that can be thousands of times more than is permitted in diesel fuel). The health impact of shipping pollution is difficult to quantify, but recent studies indicate approximately 60,000 deaths per year owing to shipping emissions with health-bills running into $Billions [7]. Schultz [25] used laboratory data for antifouling coatings in the fouled and un-fouled state [24] to estimate the change in resistance and powering for a Naval frigate, finding that heavy calcareous fouling (with roughness height of ∼10 mm or NSTM rating 90 - 100) could result in powering penalties of 86% at cruising speed. In a subsequent extension to this work [26], the economic impact of more moderate hull fouling to the US fleet of FFG-7 frigates was calculated at $1B over 15 years. When one considers that this calculation is for just 56 ships out of the 90,000 estimated to be operating worldwide [8], one realises that the net economic and environmental impact of surface roughness via biofouling on the global shipping industry is huge.

To make full-scale predictions of the performance impact of surface roughness on a wall-bounded flow we must be able to predict the increase in skin friction drag (or 'resistance to motion') due to a given surface roughness condition. The only true method to estimate the drag is (i) establish the equivalent sand-grain roughness k_s of the surface (ii) use this measure within an integral formulation of the evolving turbulent boundary layers

[1]Only superhydrophobic surfaces [23] or riblet (shark-skin) type textures [4] will give drag below smooth conditions.

which will then yield an average drag acting on the roughened surface. This methodology is explained in detail in [18]. Part (ii) of this problem is relatively well established, and follows an integral approach originally proposed by Prandtl & Schlichting [22] and later refined by [13, 14, 18]. The bottleneck in this process is part (i); the determination of equivalent sand-grain roughness. At the present time, there is no reliable methodology for determining k_s directly from a surface scan of the wall boundary under consideration (i.e the hull of a ship, fuselage of an aircraft, surface topography of the earth etc). This problem arises because the equivalent sandgrain roughness k_s, though expressed in meters, is not a directly measurable quantity of the surface topology. Rather, it is a flow quantity characterising how much effect the surface roughness has on the turbulent boundary layer, which can only be ascertained by exposing the rough surface to a flow at several different speeds (or Reynolds numbers). This often takes place in a laboratory facility, with the rough surface often being replicated for laboratory study at great cost. Other options for determining k_s are discussed later in this text. Towards the end of this paper, we describe a more direct *in-situ* method that can in principle bypass step (i) to give an immediate measure of the local drag coefficient on the hull of an operating ship. This measure can then be incorporated into step (ii) to obtain the full drag prediction for the entire hull.

It should be noted that the full-scale predictions typically require assumptions regarding the form of the mean velocity profile. The methods listed above [22, 13, 14, 18] all assume that the viscous scaled mean velocity profile $U^+(z^+)$ for the developing turbulent boundary layer over the rough wall, is similar to that of the smooth wall but with an additional downwards shift $\Delta U^+ = f(k_s^+)$ known as the Hama roughness function. Here superscript '+' denotes viscous scaling of velocity ($U^+ = U/U_\tau$) and distance ($z^+ = zU_\tau/\nu$), where U_τ is the wall drag velocity (which consists of both visocus drag and pressure drag for a rough wall), ν is the kinematic viscosity and x, y and z are the streamwise, spanwise and wall-normal directions. This shifted mean profile is often referred to as 'outer layer similarity' (after Townsend's [32] original hypothesis). The concept of outer layer similarity has important implications to our understanding of the physics of rough-wall turbulent boundary layers. However, in terms of full-scale predictions, the most important ramification of outer layer similarity is that it permits full-scale drag predictions via the assumed self-similar mean velocity profiles - see for example [22, 13, 25, 14, 18]).

Current practice for predicting the penalty on ships

A quick survey of literature from the marine coatings industry can give a feel for current practice in terms of predicting the performance penalty due to a roughened hull. According to the International Paints brochure, entitled, '*Hull Roughness Penalty Calculator*', the increase in skin friction drag due to a rough surface, as compared to a baseline or starting condition can be calculated from the following expression,

$$\Delta C_F = 0.044\left[\left(\frac{k_2}{L}\right)^{\frac{1}{3}} - \left(\frac{k_1}{L}\right)^{\frac{1}{3}}\right] \qquad (1)$$

where ΔC_F is the increase in frictional coefficient, L is the length of the vessel, k_2 is the average hull roughness (AHR) of the rough surface and k_1 is the AHR of the starting or baseline condition from which the ΔC_F is being calculated. Strictly speaking we know that for a fully rough surface, the total average skin friction C_F of a plate of length L, becomes constant for constant k/L. However, the smooth wall average skin friction resistance is a function of Re_L ($= U_\infty L/\nu$, where U_∞ is the vessel speed and ν is the kinematic viscosity of the fluid - itself a strong function of sea temperature). This is clear from the analysis of Graville [13], and more specifically from the analysis of [18] (see figure 2*a* later in this paper). Hence the only way that ΔC_F can be invariant with unit Reynolds number is if both k_1 and k_2 are in the fully rough regime. Otherwise, if k_1 is considered to be the in smooth ($k_1 = 0$) or transitionally rough regime ($k_1^+ < 70$), the analysis of Granville and others [13, 18] reveals that for constant k/L and constant plate length L, ΔC_F must be a function of k_2/L *and* unit Reynolds number U_∞/ν. Though Townsin is cited by International Paints as the source of equation (1), Townsin himself was aware of the need to include a Reynolds number term in such an expression [33].

Aside from issues of Reynolds number dependance, there are also valid questions over the manner in which the roughness height is incorporated into the drag prediction of equation (1). The two roughness heights k_2 and k_1 are defined as the average of a number of hull roughness readings of Rt_{50}, which is the maximum peak to trough roughness height in any given 50mm length recorded by a hull roughness analyser or gauge. However, the presence of k_1 and k_2 in equation (1) should provide a measure of the dynamic roughness. Detailed laboratory work has confirmed that a wide range of surface properties can contribute to the dynamic roughness height, including for example solidity [15, 17], effective slope [19, 3], average roughness height [1, 3], skewness [9] etc to name but a few. The upshot of this is that a variety of surfaces with identical peak-to-trough roughness heights could yield very different dynamic effects on the flow, and hence very different drag penalties in practice, and yet equation (1) cannot capture this complexity (returning the same ΔC_F for each). As an example of this, Schultz shows that for a set of pyramid type roughness, with identical peak-to-trough roughness height but varying effective slope (or solidity), the roughness function ΔU^+ can vary by over 50%, equivalent to a four-fold change in dynamic equivalent roughness height. The limitations of equation (1) can be judged from an example surface. The tubeworm surface analysed in [18] was found (through a modified Granville type analysis using a laboratory determined equivalent sandgrain roughness k_s) to yield a 44% increase in total averaged skin friction drag for an FPG-7 Frigate of length 124 m in cruise (7.7 ms^{-1}). Equation (1), with the measured AHR = 0.607 mm (based on average peak-to-trough roughness height over 50 mm profiles for this surface), would yield a percentage increase in total skin friction drag of 49%, which is very close to the results of [18]. However, for the same ship at full-speed (15.4 ms^{-1}), equation (1) predicts the same drag increment of 49% (owing to the lack of Reynolds number dependence), where the analysis of [18] suggests a percentage drag increment of 59%. This shows the importance of unit Reynolds number in these calculations.

Chugoku Marine Paints Ltd on the other hand, provide an alternative method of determining the increase in friction drag owing to a particular hull roughness. They produce a measure known as the Friction Increase Ratio (FIR), which gives the percentage increase in friction as a function of R_z (which is the average peak-to-trough roughness height of the surface - similar to AHR defined above) and R_{Sm} (which is the average roughness wavelength),

$$FIR(\%)\left(=\frac{\Delta C_F}{C_{F_s}}\right) = 2.62\times\frac{R_z^2}{R_{Sm}} \qquad (2)$$

Both R_z and R_{Sm} are expressed in microns and C_{f_s} is the smooth wall skin friction coefficient. This expression appears immediately dubious dimensionally, since the constant must have units (μ m $^{-1}$). Additionally, we know that the percentage increase in wall drag is a complex function of Reynolds number (again

see [18] or [13] or figure 2*b*). This is missing from equation (2), which suggests that for a given surface roughness the percentage drag increase will be the same if the ship is moving at 1 ms^{-1} or at 15 ms^{-1}. This makes little sense, since it is well established that it is not the physical roughness height in microns that determines how much effect the surface has on the flow, but rather the roughness Reynolds number, which is missing from this expression. On the plus side, equation (2) does implicitly account for the effective slope or solidity of the surface profile, both of which have been shown to influence the wall drag [15, 19, 27, 9, 3, 17] (the ratio R_z^2/R_{Sm} describes some measure of the steepness of the roughness profile). Again we might judge the limitations of equation (2) from the tubeworms experiment of [18] using the prediction for the FPG-7 Frigate of length 124 m in cruise (7.7 ms^{-1}). The AHR for this surface is 607 μm and the roughness length is $R_{Sm} = 7800$ μm (approximately 8 mm - although R_{Sm} seems like a dubious surface parameter for such a highly skewed or sparsely fouled surface). Equation (2) returns a 123% increase in skin friction coefficient for this surface, which is substantially larger than the 44% reported by [18], again this value would be entirely invariant with unit Reynolds which is contrary to the known scaling behaviour.

Direct determination of k_s^+

As stated above, in the roughness and turbulent boundary layer research communities [2], a prior determination of the equivalent sandgrain roughness k_s is considered an essential first step to predicting the full-scale drag penalty of an engineering system. Contrary to the implicit assumptions in equations (1) and (2) above, the dynamic effect of a given surface topography cannot yet be confidently measured from simple surface scan information. Below we briefly review some of the methods available to determine k_s once the surface roughness of interest has been scanned.

Experimental example

Experimentally, k_s is typically determined by exposing the rough surface to a flow and carefully measuring the friction drag coefficient C_F (or a surrogate for C_F). To obtain k_s, this must be repeated across a range of conditions until C_F (at a given x location) becomes invariant with variations in flow velocity, at which point the flow/surface is referred to as being 'fully rough'. Experimentally, there are numerous potential procedures for achieving this. If a sample of the biofouling can be obtained (or replicated) the drag, and hence k_s can be measured using tow-tank measurements, rotating disk experiments, or in wind- (or water-) tunnel facilities or fully turbulent channel or pipe facilities ([28] gives a comparison of these methods). Of these latter techniques, pipe and channel facilities are attractive, since the wall drag can be determined with good accuracy from the pressure drop in the streamwise direction [10] (although installation of the surface roughness can be difficult). For developing turbulent boundary layers, determination of C_F is typically more troublesome requiring use of drag balances [e.g. 16, 31], Reynolds shear stress measurements [e.g. 11, 34] or estimation of C_F from the shift in measured mean velocity profiles [e.g. 18]. Surfaces under test are either grown on specially prepared coupons and transferred into the lab for testing [35, 29] or the laboratory test surface can be replicated (through casting, machining, rapid prototyping or combinations) from surface scans [36, 18]. Advantages of replicated geometries are that it is not necessary to introduce fouling into sensitive experimental facilities and the surfaces can be scaled for testing at different conditions or in the case of biofouled surfaces, tested using fluids other than seawater. However, the rigid replicated surfaces preclude the evaluation of soft fouling (which are believed to move under realistic flow conditions, altering the effective roughness [30, 35]).

As an example of the experimental determination of k_s from a given scanned surface, in Figure 1 we give a brief overview of a recent study by the authors [18]. A coupon of a light calcareous tube worm fouling was obtained (Figure 1*a*), and scanned using a two axis traversing laser triangulation sensor (*b*). This surface was subsequently scaled by a factor of 1.5, made periodic in the wall-parallel directions and replicated to form a tiled test surface in a laboratory windtunnel (*c*). Detailed velocity profiles measured in the turbulent boundary layer formed over this surface permitted the Hama roughness function ΔU^+ and hence the equivalent sandgrain roughness k_s to be determined (*d*). The experimentally determined function $\Delta U^+(k_s^+)$ (shown in figure 1*e*) permits a full-scale prediction of the performance penalty due to this surface condition.

Computationally

Eventually, computational simulations may bypass the need for costly experimental determination of k_s. However, at the present time such simulations remain expensive. In order to accurately capture the effect of the roughness on the near-wall viscous dominated turbulence, high fidelity simulations are required. This will require Direct Numerical Simulations (DNS) or wall-resolved Large Eddy Simulations (LES), with body fitted meshes and relatively high Reynolds numbers. To attain the 'fully rough' condition (needed to accurately determine k_s), one would expect to require a viscous scaled equivalent sandgrain roughness (k_s^+) on the order of 70 -100. Additionally, it is generally understood that δ/k (where δ is the boundary layer thickness, channel half-height or pipe radius) should be greater than 40 [15]. Together these requirements necessitate friction Reynolds numbers $Re_\tau = \delta U_\tau/\nu > 4000$. At minimum two simulations at Reynolds numbers beyond this limit would be required to confirm that the fully rough state had been attained, and to estimate k_s for the surface. When one factors the additional computational cost due to the body meshed rough surfaces, which typically require smaller time steps and more dense grids than smooth surfaces, it is clear that these simulations are beyond the currently available computational resources for most applications. However, in the not-too-distant future computational capabilities will evolve to the point where these Reynolds numbers are well within the capabilities of engineers working on this problem. In recent years, there are increasing examples in the literature where DNS has been used to investigate realistic fouled surfaces [e.g. 2].

A promising step in this direction was recently suggested by [5], who showed that truncated domain DNS (minimal channels) could be used to accurately predict the Hama roughness function ΔU^+ of a given surface topology. It has been known for some time that a truncated DNS domain, in the spanwise direction, will constrain the turbulence, restricting the larger scales of motion. This constraint alters the flow for $z > 0.4L_y$ (where L_y is the width of the minimal span channel). Chung *et al.* [5] show that provided this domain is wide enough such that the roughness topography is fully immersed in unconstrained turbulence (provided $L_y > k/0.4$), the downward shift in the mean velocity profile ΔU^+ will be accurately captured by the minimal channel simulation. This is an interesting result, opening the way for immediate DNS characterisation of certain small-scale surfaces. As an example of the economies of this technique, Chung *et al.* show that at $Re_\tau = 950$, a minimal channel simulation can yield the same result for ΔU^+ as the full channel simulation in a fraction ($1/60^{\text{th}}$) of the CPU hours, and

[2] although perhaps less so in the biofouling, maritime communities

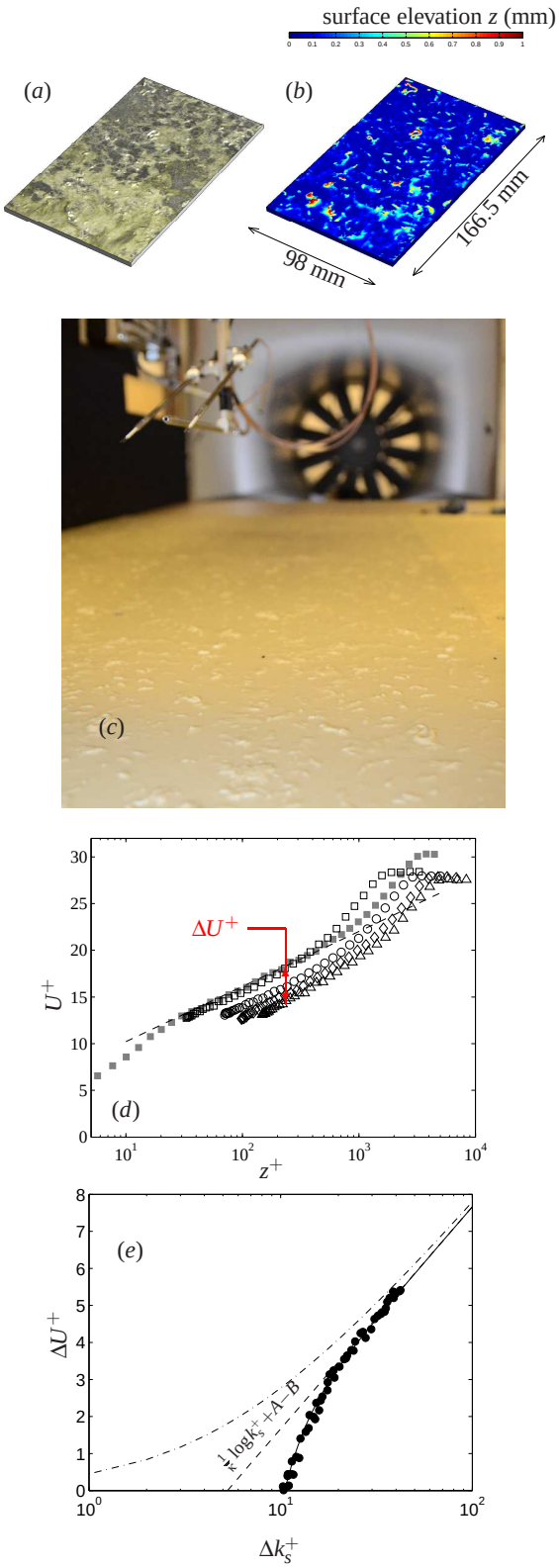

Figure 1: (*a*) Photograph of the fouled tube-worm coupon ; (*b*) The laser surface scan, with the colour scale showing the elevation height of the surface topology; (*c*) replicated surface installed in wind-tunnel; (*d*) mean velocity profiles over the rough surfa ce; (*e*) ΔU^+ as a function of k_s^+.

with a number of grid points that is three orders of magnitude less than the full domain simulation. There remain limitations to this technique. The numerical domain must be sufficiently wide such that it contains a statistically representative sample of the surface, hence the advantage of the minimal channel approach will diminish in cases where the roughness has a large-scale characteristic spanwise wavelength, or in situations where there is large-scale spanwise heterogeneity. However for roughness which has a relatively small repeating scale in the wall parallel dimension, such as topologies due to machining / manufacturing processes and painting or spraying, this technique could be an attractive new method for characterising k_s and permitting full-scale drag predictions.

Correlations

The ultimate goal for roughness research would be to bypass these costly experimental and numerical steps for obtaining k_s, and instead formulate functions that enable a direct calculation of the equivalent sandgrain roughness given some easily measured properties of the surface (such as root-mean-square roughness height, effective slope, skewness etc). The database of results for different rough surfaces has been steadily growing since Nikuradse's pioneering sandgrain experiments, and this growing compendium of results have aided the formulation of certain empirical relationships along these lines. Flack & Schultz [9] give a comprehensive overview of these. Many of these predictive methods work reasonably well for the surfaces on which they were formulated (e.g. painted surfaces, cast or honed surfaces etc.). However, none seem to be applicable across the wide range of roughness geometries that can be encountered in marine / aerospace / atmospheric flows.

Progress does seem to be being made in terms of identifying key surface parameters that govern the influence of a given surface topography on the flow (and hence the influence on k_s). Perhaps most revealing in this respect are studies where individual roughness parameters have been systematically investigated, in controlled experiments, with other parameters remaining fixed. Examples here could be the systematic study of effective slope in [19, 27, 3], or the related study of solidity in [17]. All studies seem to convincingly demonstrate that some measure of solidity/effective slope and roughness height would be a bare minimum requirement for an effective correlation [3].The effect of frontal and plan solidities have been investigated in a similarly systematic fashion [21]. In the future, it is likely that DNS will play a key role in these systematic studies, where it is relatively straight forward to systematically vary a mathematically generated surface, and where the uncertainties in determining the wall drag are often much lower than in experiments. Indeed Macdonald *et al.*'s [17] study of solidity used the minimal channel DNS methodology discussed above, to study surfaces in the dense (high solidity) regime. At present these systematic studies certainly do not cover the full range of parameters that have proven to be of relevance. Studies have also suggested that skewness, kurtosis and other roughness density measures are required parameters in formulating accurate correlations [9]. As a final remark, the challenge to assimilating all of these previous attempts at correlation and systematic study is that many of these surface parameters can be inter-related in non-trivial ways. This is also exacerbated by a tendency for incomplete characterisation of the surfaces under test within existing literature. Despite 80 years of quite extensive research since Nikuradse's seminal study, it is probably fair to say that the compendium of adequately documented results is not as large as it could be. All too often, surfaces have been characterised in terms of just one or two key parameters, where in fact a more complete surface scan information would have greatly enhanced the prospects of meaningful comparison between studies and the eventual formulation of more effective correlations. The numerical and experimental sections above will give a feel for the expense and

effort involved in determining k_s for a given surface. Given this outlay, it would seem prudent for the community to ensure that these results can also contribute to the development of improved correlations, by ensuring that key surface parameters and preferably full surface scan data are made available.

Drag due to ZPG-TBL on a roughnened flat plate

Predicting the drag on a roughened flat plate is considerably more complicated than for an internal fully turbulent flow (pipe or channel). In internal geometries, in the fully rough case, the skin friction coefficient becomes constant for a given k_s/D (where D is the diameter of the pipe or half-height of the channel). Since D is invariant with length for a pipe or channel, this condition is satisfied for a uniformly distributed roughness. For the developing TBL case, it is easy to show algebraically that the local skin friction coefficient only becomes constant when k_s/δ becomes constant. For the developing TBL the boundary layer thickness δ will grow with distance x along the flat plate, and hence for a uniformly distributed roughness, k_s/δ will reduce with x, and hence C_F will not be constant along the plate.

Based on an assumed mean velocity profile for a turbulent boundary layer formed over a rough wall, and also the momentum integral equation, it is possible to predict the local skin friction coefficient C_F as a function of distance along a flat plate. This analysis has been outlined analytically in [22, 13], while a numerical approach to the same problem was sought in [18]. the advantage of the numerical approach is that it is easy to incorporate different wake functions, and also more complex functions of $\Delta U^+(k_s^+)$, whilst the analytical approaches have the advantage that the resulting algebraic solutions can lay bare the scaling parameters. We will here give a brief description of the approach following the numerical scheme suggested in [18]. The mean viscous scaled velocity profile $U^+(z^+)$ for the smooth wall boundary layer is typically considered to consist of an inner region profile, a logarithmic region, and also a wake profile [e.g. 6]. In the case of the rough wall boundary layer, the entire profile is considered to be shifted downwards by the Hama roughness function ΔU^+. At high Reynolds numbers, the inner part of the profile contributes insignificantly to the overall drag on the flat plate, and therefore we could model the mean profile as follows,

$$U^+ = \underbrace{\frac{1}{\kappa}\log z^+ + A}_{\textit{log region}} \quad \underbrace{-\ \Delta U^+}_{\textit{roughness function}} \quad + \underbrace{\frac{\Pi}{\kappa} W\left(\frac{z}{\delta}\right)}_{\textit{wake function}} \tag{3}$$

where Π is the wake strength and W is the wake function (a function of z/δ; typically small for $z/\delta < 0.15$ and equal to 1 for $z = \delta$). The roughness function ΔU^+ could be any function of k_s^+, however for brevity here we will assume the fully rough form,

$$\Delta U^+ = \frac{1}{\kappa}\log k_s^+ + A - B \tag{4}$$

Substituting this expression into equation 3 and making use of the relationship that when $z^+ = \delta$, $U^+ = U_\infty/U_\tau = \sqrt{2/C_F}$, (where C_F is the local skin friction coefficient $= 2\tau_w/\rho U_\infty^2$ and U_τ is the wall drag velocity $= \sqrt{\tau_w/\rho}$) gives,

$$\sqrt{\frac{2}{C_F}} + \frac{1}{\kappa}\log\sqrt{\frac{C_F}{2}} = \frac{1}{\kappa}\log\delta^+ - \frac{1}{\kappa}\log\frac{k_s U_\infty}{\nu} + B + \frac{\Pi}{\kappa}W\left(\frac{z}{\delta}\right) \tag{5}$$

For this equation, if B, κ and Π are assumed to be constants, and if we know k_s, the wake parameter W and the operating conditions for the system (U_∞ and ν), then there is a unique relationship between δ^+ and C_F. The numerical procedure outlined in [18] effectively assumes a range of δ^+ values from very low O(100) to beyond the maximum we would expect on the system under consideration O(1×10^6). For this range of δ^+ values, equation (5) will return a corresponding local skin friction coefficient C_F. The assumed value of δ^+ also uniquely defines the mean velocity profile $U^+(z^+)$ from equation 3 which can then be used to calculate the Reynolds number based on momentum thickness ($Re_\theta = \theta U_\infty/\nu$, where θ is the momentum thickness) using the following relationship,

$$Re_\theta = \int_0^{\delta^+}\left(U^+ - \sqrt{\frac{C_F}{2}}U^{+^2}\right)dz^+ \tag{6}$$

At this stage, for the guessed values of δ^+, the parameters C_F and Re_θ are also known. However the x location along the flat

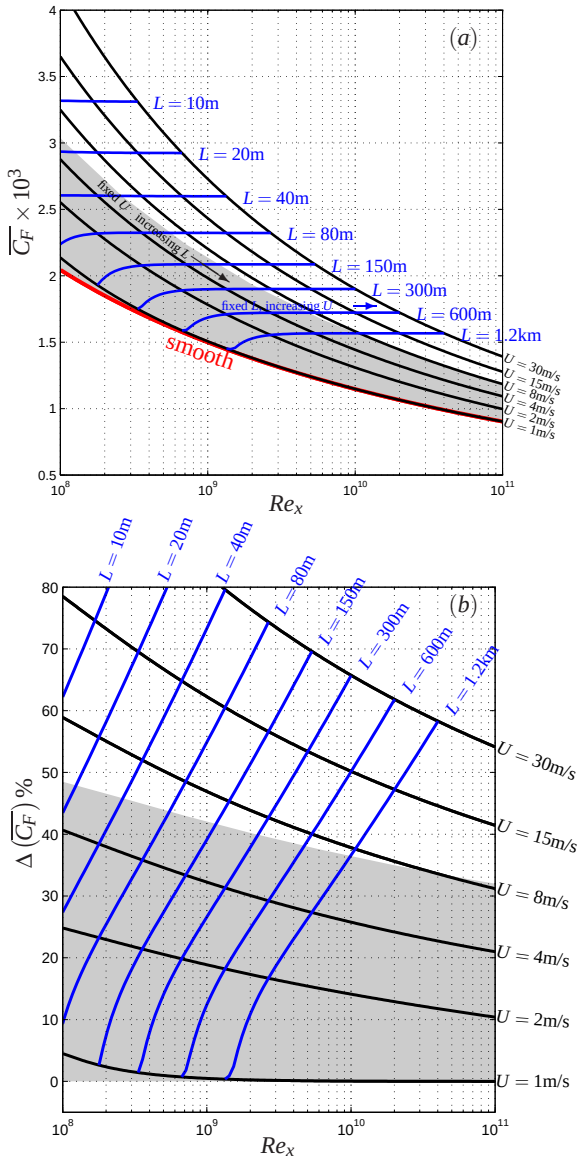

Figure 2: (a) Predicted average skin friction coefficient curves for a flat plate. The red curve shows the smooth case, blue and black curves show lines of constant unit Reynolds number U_∞/ν and lines of constant length respectively for the roughened tube worms case of [18]. (*b*) percetage increase in $\overline{C_F}$ relative to the smooth case for the same rough surface. Gray shaded region shows transitional roughness regime.

plate at which these δ^+ values are attained is as yet unknown. To solve this, we make use of the mean momentum integral equation to assume that,

$$Re_x = \int \frac{2}{C_F} dRe_\theta \tag{7}$$

which when solved (numerically in the case of [18]) will yield the associated x location for each assumed value of δ^+. This procedure gives the local skin friction coefficient C_F as a function of distance along the plate, from which the total integrated skin friction for the plate $\overline{C_F}$ can be easily calculated,

$$\overline{C_F} = \frac{2Re_\theta}{Re_x} \tag{8}$$

Typically, we are most interested in the percentage or fractional increase in $\overline{C_F}$ due to a particular roughness, over and above the smooth or some other baseline case. The above methodology will also yield the smooth wall $\overline{C_F}(x)$ if the Hama roughness function is discarded from equations (3) and (5). Using this methodology, for a given pre-characterised roughness (as detailed in the section above), we can produce a chart such as those shown in figure 2 that can assist in making the full-scale predictions. The blue lines in figure 2 show lines of constant plate length L, the black lines show lines of constant unit Reynolds number U_∞/ν, which if we assume a constant kinematic viscosity $\nu = 8.97 \times 10^{-7} \mathrm{m^2 s^{-1}}$ equates to the freestream velocities indicated on the figures. Figure 2(a) shows $\overline{C_F}$ as a function of Re_x. The grey shaded regions show the transitionally rough regime. In this region, the results are specific to the measured $\Delta U^+ = f(k_s^+)$ curve as determined for the tube worms surface by [18]. However in the fully rough regime, the blue horizontal lines in 2(a) would be universal for a given k_s/L (the k_s for the tube worms surface is 325 μm). Beyond the grey shaded region, the black lines are universal lines of constant $k_s U_\infty/\nu$. Figure 2(b) reformats the data from plot (a) as a percentage increase in average skin friction coefficient $\overline{C_F}$ compared to the smooth case, as given by

$$\Delta\overline{C_F}(Re_x)\% = 100 \times \frac{|\overline{C_F}(Re_x)|_r - |\overline{C_F}(Re_x)|_s}{|\overline{C_F}(Re_x)|_s} \tag{9}$$

where subscripts r and s refer to the rough and the smooth condition respectively. Note from this plot that for both lines of constant U and lines of constant L, that $\Delta\overline{C_F}\%$ is always a function of Reynolds number, hence highlighting the short-comings in the simplified prediction methods given by equations (1) and (2). Note also, that for a given roughness, if the flat plate were long enough, the solution for $\overline{C_F}$ would eventually collapse back to the smooth case. This is clear from the curve for $U_\infty = 1$ $\mathrm{ms^{-1}}$, which for the given surface presented would collapse to the smooth condition if $Re_x > 10^9$, which corresponds to a length of approximately 1 km. This scenario is unlikely to be relevant to any marine / aerospace applications. (for a cruising speed beyond 1.9 $\mathrm{ms^{-1}}$, the flat plate would need to be longer that the circumference of the earth for $\Delta\overline{C_F}$ to be less than 1%). Of more use, it is clear from figure 2(a) that for the fully rough flow, the average skin friction coefficient becomes constant for a fixed L (with varying unit Reynolds number). However, figure 2(b) shows that in this regime, the percentage change in $\overline{C_F}$ remains a strong function of Reynolds number, contrary to the implications of equations (1) and (2).

Full-scale sea-trial

Given the difficulties and expense associated with making an accurate drag prediction based on a given surface roughness

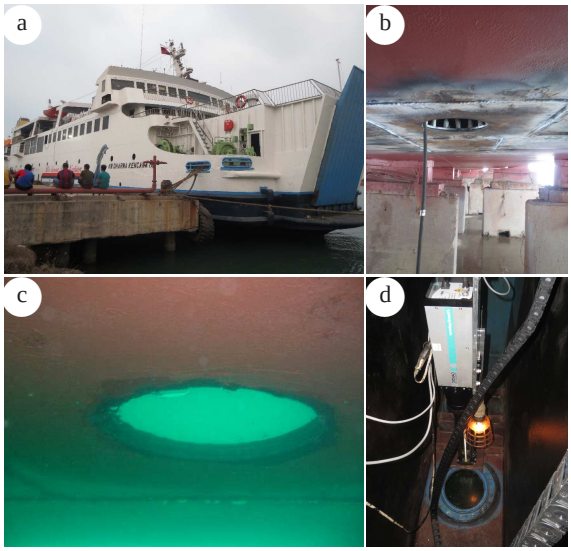

Figure 3: (a) The ship Dharma Kencana IX, kindly provided by PT. Dharma Lautan Utama, entering dry dock at Cilegon, Indonesia; (b) hole is cut in the hull for installation of optical access; (c) underwater photograph of installed window obtained during dive inspection; (d) The Dantec FlowExplorer Laser Doppler Anemometer installed on the traverse in the enclosure between the hulls. The inside of the installed window is also visible in this image.

observation, we here detail preliminary work that attempts to make a direct prediction of the drag penalty of a ship due to hull roughness, through *in situ* boundary layer measurements over the hull of an operating ship. The assumption here is that a measure of the velocity gradient in the logarithmic region of the turbulent boundary layer, formed over the hull of an operating ship, should be sufficient to directly estimate the drag. This assumption is based on the differentiated equation for the mean viscous scaled velocity profile within the logarithmic region of a turbulent boundary layer,

$$U^+ = \frac{1}{\kappa}\log z^+ + A - \Delta U^+ \tag{10}$$

from which (since A and ΔU^+ are not functions of z^+) we get,

$$\begin{aligned} \frac{dU^+}{dz^+} &= \frac{1}{\kappa z^+} \\ U_\infty\sqrt{\frac{C_F}{2}} &= \kappa z \frac{dU}{dz} \end{aligned} \tag{11}$$

The wall-normal distance z for a rough wall is the distance from the crest of the roughness z_r plus ε (an offset to account for the virtual origin). With sufficient measurements at known wall-normal locations within the log region, it is possible to determine U_τ and hence C_F from a velocity profile obtained in the logarithmic region. This will afford a direct measure of the local skin friction on the operating ship. The plan here is to use a Dantex FlowExplorer Laser Doppler Anemometer, looking outwards through a small window installed in the bottom of the hull of a ship. Our partners in this project, PT. Dharma Lautan Utama (an Indonesian ship owner/operator) kindly granted permission for this window to be added to the RO/RO passenger ferry Dharma Kencana IX during dry-docking. During annual dry-docking and scheduled hull cleaning in Cilegon, Indonesia, a window was installed on the underside of the hull, approximately 25 m downstream of the bow of the ship. A water-tight

Roughness parameter	value	units	Formula
			—
k_a	0.035	mm	$\overline{\lvert z' \rvert}$
k_{rms}	0.045	mm	$\sqrt{\overline{z'^2}}$
k_p	0.510	mm	$\max z' - \min z'$
k_{sk}	0.030	–	$\overline{z'^3}/k_{rms}^3$
k_{ku}	3.253	–	$\overline{z'^4}/k_{rms}^4$
ES_x	0.087	–	$\overline{\left\lvert \frac{dz'}{dx} \right\rvert}$

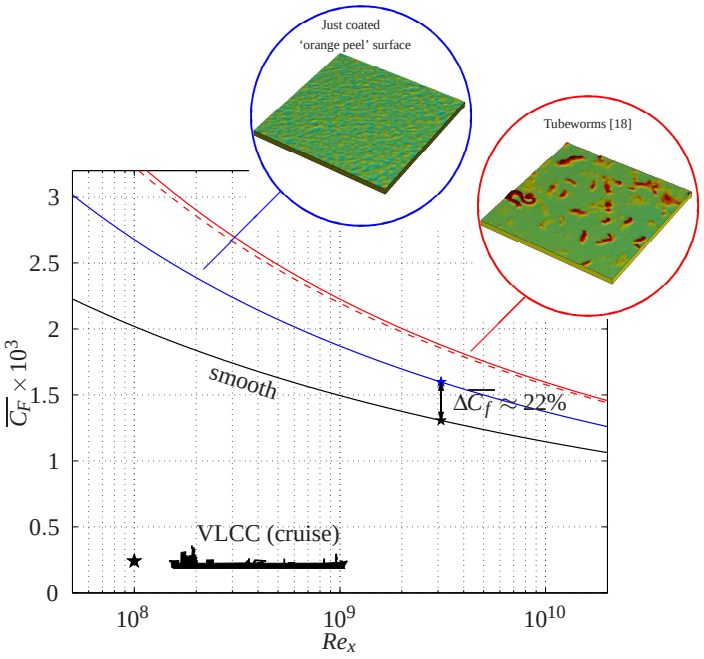

Figure 4: Tabulated surface parameters for the scanned 'orange peel' just-coated hull condition. Graph shows average skin friction coefficient $\overline{C_F}$ against Reynolds number Re_x for the (black line) smooth surface and (solid red line) the tubeworm surface with the experimentally determined $k_s = 325$ μm from [18]; (red-dashed curve) shows the tube-worms predicted $\overline{C_F}$ based on the measured surface parameters and the correlation of [3]; (blue curve) shows the predicted $\overline{C_F}$ for the just-painted surface finish on the Dharma Kencana IX based on measured surface parameters and the correlation of [3]. Symbols show operating points for a very large crude carrier for ($\star$) smooth and ($\star$) 'just-coated' conditions.

enclosure was welded in position between the double hull to house the measurement equipment, consisting of the LDA and computer controlled traversing rail. This enclosure ensures the integrity of the ship in the unlikely event of a window failure. The LDA measurement will be complemented with regular dive inspections and underwater surface scanning (using an image based tomographic reconstruction technique). It is planned that the resulting scanned surfaces will be scaled and replicated for wind tunnel testing following the technique outlined above and in [18]. These laboratory measurements will provide validation of the LDA gradient-based technique for *in-situ* direct determination of the local skin friction coefficient.

During dry docking, surface impressions were made of the freshly coated ship to provide a baseline record of the surface, prior to the expected build-up of bio-fouling during operation. This surface imprint has been scanned using a two-axis traversing laser triangulation sensor in the laboratory at the University of Melbourne. The resulting scanned topology is shown in the inset of Figure 4. The surface finish is highly dependant on the degree of hull preparation prior to re-coating, (which in this instance was sweep blasted to remove previous fouling, rather than fully cleaned back to bare metal), and also the spraying process itself. The resulting 'orange peel' type surface finish had an average roughness height $k_a = 35$ μ m, with effective slope $ES_x = 0.087$. Full parameters are tabulated in figure 4. As discussed previously in this paper, there currently lacks a reliable methodology to enable k_s to be directly predicted from surface scan information. Ultimately we will conduct detailed laboratory turbulent boundary layer measurements over the scaled and replicated 'orange peel' surface to determine the drag penalty (following the methodology of [18]). However, in the interim, a preliminary estimation of the drag penalty due to this surface can be estimated from the correlation suggested by [3], who demonstrated that a formulation based on k_a^+ and ES_x could be effective at predicting the roughness function ΔU^+ for a wide range of surfaces. This correlation yields results for the tube worm surface of [18] that are in close agreement to the experimentally determined values. The red curve of figure 4 shows the predicted $\overline{C_F}(Re_x)$ for tube worms surface using the experimentally determined $\Delta U^+(k_s^+)$ (from [18]). The red dashed line shows the prediction using the correlation $\Delta U^+(k_a^+,\, ES_x)$ from [3] demonstrating very good agreement. Based on this, the same correlation is used to predict $\overline{C_F}(Re_x)$ for the observed 'orange peel' baseline surface (shown by the blue curve). The star symbols indicate the operating point for the VLCC discussed in [18], indicating that for this type of large bulk carrier the base-line (fresh from dry dock) surface finish could already produce a 20% drag penalty compared to the ideal dynamically smooth case.

Conclusions

The case of a turbulent boundary layer developing over a rough surface is discussed. Particular attention is given to how full-scale predictions of the drag penalty can be obtained in such scenarios (including a review of current practise in the maritime industry). Determining the dynamic roughness height is the bottle-neck in the process of obtaining accurate predictions, and several methods to achieve this are discussed. Finally, a novel experiment is introduced, that should enable direct *in situ* measurement of the local drag coefficient on the hull of an operating ship. Initial results from this study indicate that the 'just-coated' baseline hull condition, in the absence of any fouling, may already represent a substantial drag penalty over the dynamically smooth ideal.

Acknowledgements

The authors would like to thank the Australian Research Council, the Newton Fund and the Australia Indonesia Center for support of this work. Gratitude is also extended to Dr Marcus Tullberg of Hempel A/S, PT. Dharma Lautan Utama and Biro Klasifikasi Indonesia (BKI).

References

[1] M. Acharya, J. Bornstein, and M. P. Escudier. Turbulent boundary layers on rough surfaces. *Exp. Fluids*, 4:33–47, 1986.

[2] A. Busse, C. J. Tyson, and N. D. Sandham. Direct numerical simulation of turbulent channel flow over engineering rough surfaces. In *Proceedings of the eighth International Symposium on Turbulence and Shear Flow Phenomena*, 2013. TSFP8, Poitiers, France.

[3] L. Chan, M. MacDonald, D. Chung, N. Hutchins, and A. Ooi. A systematic investigation of roughness height and wavelength in turbulent pipe flow in the transitionally rough regime. *J. Fluid Mech.*, 771:743–777, 2015.

[4] K.-S. Choi. Near-wall structure of a turbulent boundary layer with riblets. *J. Fluid Mech.*, 208:417–458, 1989.

[5] D. Chung, L. Chan, M. MacDonald, N. Hutchins, and A. Ooi. A fast direct numerical simulation method for characterising hydraulic roughness. *J. Fluid Mech.*, 773:418–431, 2015.

[6] D. Coles. The law of the wake in the turbulent boundary layer. *J. Fluid Mech.*, 1:191–226, 1956.

[7] J. J. Corbett, J. J. Winebrake, E. H. Green, P. Kasibhatla, V. Eyring, and A. Lauer. Mortality from ship emissions: A global assessment. *Environ. Sci. Technol.*, 41(24):85128518, 2007.

[8] V. Eyring, I. Isaksen, T. Berntsen, W. J. Collins, J. J. Corbett, O. Endresen, R. G. Grainger, J. Moldanova, H. Schlager, and D. S. Stevenson. Transport impacts on atmosphere and climate: Shipping. *Atmos. Environ.*, 44(37):4735–4771, 2010.

[9] K. A. Flack and M. P. Schultz. Review of hydraulic roughness scales in the fully rough regime. *J. Fluids Eng.*, 132:041203, 2010.

[10] K. A. Flack and M. P. Schultz. Roughness effects on wall-bounded turbulent flows. *Phys. Fluids*, 26:101305, 2014.

[11] K. A. Flack, M. P. Schultz, and T. A. Shapiro. Experimental support for townsends reynolds number similarity hypothesis on rough walls. *Phys. Fluids*, 17:035102, 2005.

[12] M. I. Goldhammer and B. R. Plendl. Surface coatings and drag reduction. Technical Report QTR_01, Boeing, Aero, 2013.

[13] P. S. Granville. The frictional resistance and turbulent boundary layer of rough plates. Technical Report 1024, Navy Department, 1958.

[14] ITTC. The resistance committee - final report and recommendations to the 25th ITTC. In *Proc. 25th International Towing Tank Conference*, 2008. Fukoaka.

[15] J. Jiménez. Turbulent flows over rough walls. *Annu. Rev. Fluid Mech.*, 36:173–196, 2004.

[16] P.-Å. Krogstad and V. Efros. Rough wall skin friction measurements using a high resolution surface balance. *Intl J. Heat Fluid Flow*, 31(3):429–433, 2010.

[17] M. MacDonald, L. Chan, D. Chung, N. Hutchins, and A. Ooi. Turbulent flow over transitionally rough surfaces with varying roughness densities. *J. Fluid Mech.*, page In Press, 2016.

[18] J. P. Monty, E. Dogan, R. Hanson, A. J. Scardino, B. Ganapathisubramani, and N. Hutchins. An assessment of the ship drag penalty arising from light calcareous tubeworm fouling. *Biofouling*, 2015. In Press.

[19] E. Napoli, V. Armenio, and M. De Marchis. The effect of the slope of irregularly distributed roughness elements on turbulent wall-bounded flows. *J. Fluid Mech.*, 613:385–394, 2008.

[20] J. Nikuradse. Gesetzmassigkeiten der turbulenten stromung in glatten rohren. *Forsch. Auf Dem Gebiet des Ingen.*, 3:1–36, 1932.

[21] M. Placidi and B. Ganapathisubramani. Effects of frontal and plan solidities on aerodynamic parameters and the roughness sublayer in turbulent boundary layers. *J. Fluid Mech.*, 782:541–566, 2015.

[22] L. Prandtl and H. Schlichting. The resistance law for rough plates. Technical Report 258, Navy Department, 1955. Translated by P. Granville.

[23] J. P. Rothstein. Slip on superhydrophobic surfaces. *Annu. Rev. Fluid Mech.*, 42:89–109, 2010.

[24] M. P. Schultz. Frictional resistance of antifouling coating systems. *J. Fluids Eng.*, 126:1039, 2004.

[25] M. P. Schultz. Effects of coating roughness and biofouling on ship resistance and powering. *Biofouling*, 23:331–341(11), 2007.

[26] M. P. Schultz. Economic impact of biofouling on a naval surface ship. *Biofouling*, 27:87–98, 2011.

[27] M. P. Schultz and K. A. Flack. Turbulent boundary layers on a systematically varied rough wall. *Phys. Fluids*, 21:015104, 2009.

[28] M. P. Schultz and A. Myers. Comparison of three roughness function determination methods. *Exp. Fluids*, 35:372–379, 2003.

[29] M. P. Schulz and G. W. Swain. The effect of biofilms on turbulent boundary layers. *ASME J. Fluids. Eng.*, 121/45:44–51, 1999.

[30] M. P. Schulz and G. W. Swain. The influence of biofilms on skin friction drag. *Biofouling*, 15:129 – 139, 2000.

[31] D. T. Squire, C. Morrill-Winter, N. Hutchins, M. P. Schultz, J. C. Klewicki, and I. Marusic. Comparison of turbulent boundary layers over smooth and rough surfaces up to high reynolds numbers. *J. Fluid Mech.*, 795:210–240, 2016.

[32] A. A. Townsend. *The Structure of Turbulent Shear Flow*. Cambridge University Press, 1956.

[33] R. L. Townsin. The ship hull fouling penalty. *Biofouling*, 19:9–15, 2003.

[34] R. J. Volino, M. P. Schultz, and K. A. Flack. Turbulence structure in rough- and smooth-wall boundary layers. *J. Fluid Mech.*, 592:263–293, 2007.

[35] J.M. Walker, J.E. Sargison, and A.D. Henderson. Turbulent boundary-layer structure of flows over freshwater biofilms. *Exp. Fluids*, 54:1–17, 2013.

[36] Y. Wu and K. T. Christensen. Outer-layer similarity in the presence of a practical rough-wall topography. *Phys. Fluids*, 19:085108, 2007.